

NANOINDENTATION ON MICRO PILLARS FOR DETERMINATION OF INTRINSIC HARDNESS AND RESIDUAL STRESS IN COATINGS DEPOSITED ON COMPLEX GEOMETRIES

B. ANDRÈ, P. HOLLMAN, and U. WIKLUND

Applied Materials Science, The Ångström Laboratory, Uppsala University

Corresponding author: Urban.Wiklund@angstrom.uu.se, tel: +46-18-4713092

Postal address: Engineering Science, Uppsala University, Box 534, SE-751 21 Uppsala, Sweden

ABSTRACT

In this work a procedure to assess the local residual stress in coatings deposited on complex substrate geometries is described. A focused ion beam (FIB) is used to mill structures small enough to relax from residual stress. Nanoindentation is used to measure the change in mechanical properties, most importantly the hardness, in relaxed coating and in as-deposited coating. This change is then related to the residual stress in the coating. This relationship can then be used to calculate the residual stresses, at other positions or at other components, from changes in hardness as measured as before.

The procedure is demonstrated on two different PVD coatings; one TiN coating and one nanocomposite TiNiC coating. On a large high speed steel substrate the TiN was measured to a hardness of 28 GPa using conventional techniques. Using this procedure, this could be divided into 23 GPa of intrinsic hardness and an extra 5 GPa induced by the known compressive residual stress of 3.9 GPa. When the same coating was deposited on a thin wire the full procedure allowed the residual stress to be determined to 3.5 GPa in compression.

INTRODUCTION

When a thin coating is deposited for example with Physical Vapour Deposition (PVD) the mechanical properties and its wear resistance is depending both on its intrinsic properties and its residual stress condition. Residual stresses can occur through differences in thermal expansion of the substrate material and the coating during cooling, through ion bombardment during deposition or due to epitaxial growth. Many thin coatings in mechanical applications are ceramic and have lower thermal expansion than the substrate material, this usually results in a compressive stress in the coating. The reason for the compressive stress is that the coating is deposited on the substrate when the system is warm. When the system then is cooled down to room temperature the substrate contracts

more than the coating, creating residual compressive stresses in the coating.

High residual stresses can be either beneficial or detrimental for a coated component. As an example, compressive residual stresses give the coating a higher resistance to plastic deformation and cracking, meaning that a coating with high compressive residual stresses has a higher lateral yield stress and higher toughness than the same coating without stress or with tensional lateral stress [1]. This can be positive if the hardness or toughness is the determining factor for the wear resistance. High compressive stresses can also be detrimental considering for example the adhesion of the coating to the substrate [2, 3].

The ability to investigate a coating both by its apparent properties and its intrinsic properties

is very interesting when new coatings are developed. Since apparent properties are influenced by *e.g.* geometry, substrate etc. it is important from a coating design point of view how the intrinsic properties change when the coating is deposited on *e.g.* small geometries such as thin wires, cutting edges, etc. Also the possibility to investigate residual stress variations at specific areas of a coated component is interesting.

One common method used today for investigations of residual stresses in coatings is XRD. In this method the changes in lattice parameter in directions going from normal to parallel to the surface is studied. This requires the coating to be crystalline, peaks that do not overlap with peaks from the substrate and a specimen of sufficient size. Moreover, it is not easily conducted on samples having a curvature.

Another method for residual stress investigation is to cut out a piece of the coating together with some substrate, glue the piece with the coated side to a plane stiff surface, remove material from the substrate side of the sample by grinding and polishing until the ratio of the coating thickness and the remaining substrate thickness is about 1/100. After this, the glue is removed, and the residual stress relaxes by bending the sample to a curvature. By measuring the curvature, the residual stress can be calculated using Stoney's equation [4, 5]. This method is applicable also to non-crystalline coatings. The problem with this method is that the sample has to be flat and, for easy handling, quite a large specimen is needed. Moreover, the preparation is difficult, especially if the coating thickness is small, and any interlayers between the substrate and coating will influence the measurement.

The method proposed in this work uses nanoindentation to determine the residual stress. To use indentations for residual stress determination has been suggested earlier [6-9] but most often the applicability of the

methods become limited for coatings deposited on complex geometries are of interest. One method and that deserves mentioning in this context is *e.g.* the work by Suresh and Giannakopoulos [6] where the effect of an equibiaxial stress state is modelled as a hydrostatic stress plus a uniaxial compressive stress component requiring a different force during indentation. Another is the work by Tsui et al. which describes experiments from indentation in aluminium [7]. The nanoindentation procedure and especially the question of contact area determination are in focus. In this work also the influence of residual stress on elastic modulus is studied although they conclude that significant procedural problems in area measurements is likely the major cause for the difference they measured in elastic modulus. A number of investigations also employ FEM calculations to model the influence of stress on hardness. One representative example of this is the work by Huber et al. [8]. All the above mentioned methods have problems when used for thin coatings with compressive residual stress. The most serious problem is the requirement to find representative, stress relieved parts of coating on small components or components on complex geometries.

Proposed procedure

The proposed method in this work is to use a focused ion beam to cut through the coating down to the substrate to create micrometer sized stress relieved pillars of coating. For a coating with unknown properties, this is done on the coating when deposited on a flat substrate that allows also deflection based measurements of the stress. Then the local intrinsic hardness is measured using nanoindentation.

The hardness of the coating in the stress relieved columns is compared to the hardness of as-deposited, stress containing coating. This difference is then compared to the

residual stress, as calculated using deflection and Stoney's equation.

This provides a relation between hardness increase and the residual stress.

This relation can, to a first approximation, be assumed to be linear as suggested by Lee and Kwon [9] and Karlsson et al. [10]. This linear relation can, together with a hardness difference between stress relieved and as-deposited coating on the real component be used to calculate the residual stress when deposited on the real component. Thanks to the small lateral surface needed for these measurements, the residual stress can be determined locally with high lateral resolution and the component itself can now be allowed to be small in size or complex in shape. Other advantages are that the coating does not have to be crystalline and interlayers have no influence on the results.

This refined method is demonstrated and compared with results from measurements using Stoney's equation on two flat samples; TiN coating deposited on High Speed Steel (HSS) and a nanocomposite coating, nc-TiNiC/a-C, deposited on nickel. The TiN

coating was chosen because it is a thoroughly investigated material known for its stability in composition and properties. The nc-TiNiC/a-C coating, on the other hand, is known to change properties with small differences in deposition parameters [11].

EXPERIMENTAL

Materials and geometry

Four different coating/substrate systems were used in this investigation. As shown in Table I, two PVD coatings, TiN and nanocomposite Ti-Ni-C, were deposited on large flat substrates, made of high speed steel (HSS) and nickel, respectively. This was to enable pillar preparation and hardness measurements as well as sample preparation for stress calculations using Stoney's equation on the very same samples. Two additional coatings, TiN and TiNiC were then deposited on thin stainless steel wires to find out if the method was applicable also for stress assessment on coatings deposited on complicated substrates.

Table I. Properties of the coating/substrate systems studied. Compositions are correct to within 2% and coating thickness on flats to within 10%. Coating thicknesses on wire is only an indication.

Coating	Composition %	Thickness	Substrate geometry	Substrate material
Ti-Ni-C	Ti:44, Ni:13, C:43	0.96 μm	Flat, \varnothing 30 mm, t=5 mm	Ni
TiN	Ti:50, N:50	5.7 μm	Flat, 20 \times 20 mm, t=5 mm	HSS
Ti-Ni-C	Ti:46, Ni:4, C:50	About 1 μm	Wire (\varnothing 0.5 mm)	Stainless steel
TiN	Ti:50, N:50	About 1 μm	Wire (\varnothing 0.5 mm)	Stainless steel

Production of stress free micro pillars

Using FEM calculations the free standing pillars were simulated to show to what extent the pillars were relieved from stress. The

stress was modeled in SolidWorks as a thermal stress resulting from an imposed increase in temperature, and the differences in thermal expansion and elastic properties between the coating and the substrate. The

results, in terms of the level of principal stress along the surface, as shown in Fig. 1, suggested that an aspect ratio, *i.e.* height/width of the pillars, should be no less than 2 in order to have fully stress relieved coating material in the top of the pillars although the highest stresses remain only below a ratio of 0.5. For the pillars in this work a ratio of at least 0.5 was aimed at.

In order to create stress free pillars of the coatings a combined Scanning Electron Microscope (SEM) with a Focused Ion Beam (FIB) Strata DB235 from FEI was used to selectively mill through the coating until the substrate was reached. The pattern used for the selective milling gave free standing pillars with close to vertical sides, sufficient height and almost untouched top surfaces. The coating of the remaining pillars expands and became free from residual stress as the milling proceeded. An example of the milling progress of TiN is shown in Fig. 2.

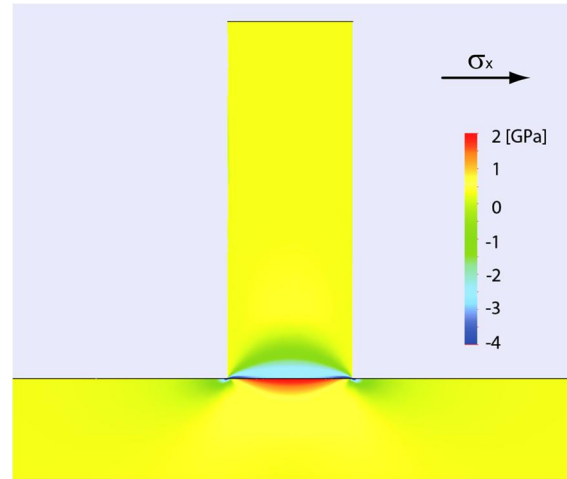


Figure 1. The principal stress σ_x in a pillar cut out from a coating with an original residual stress of 3.9 GPa. The major part of the stress is relaxed in the pillar, except close to the interface. An aspect ratio less than 0.5 would mean significant comp-repressive residual stress remains in the pillar.

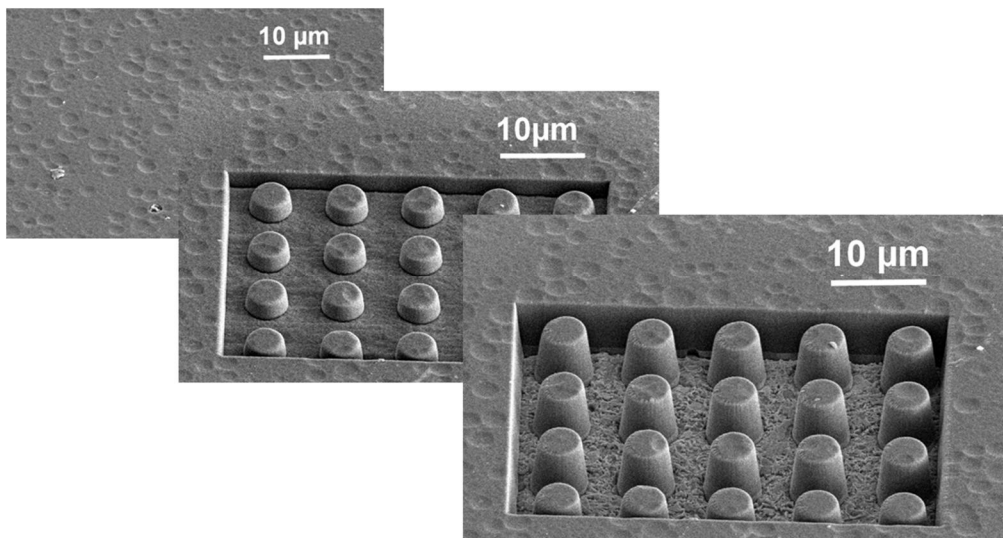


Figure 2. The progress during milling of a TiN coating to create free standing pillars without residual stress.

For the tests in this investigation the radius of the pillars was chosen to be about 2 μm . This was to assure easy positioning of nanoindentations in the middle of the pillars. A beam current of only 5000 pA was chosen to create smooth surfaces on the pillars.

Hardness measurement

Nanoindentation was used to measure the hardness of both as-deposited coating, at least 100 μm away from the FIB-pattern, and of the pillars which constitutes stress relieved coating. The nanoindentations were performed in an UNHT system from CSM Instruments equipped with a Berkovich diamond tip and the indentation curves were analysed using the Oliver and Pharr procedure [12]. The indentations were conducted to a maximum depth of 30 nm to avoid influence from both the substrate and the periphery of the pillars.

Residual stress using deflection measurements

The stress in the coatings on the flat substrates was measured using the conventional method using Stoney's equation. For these tests quadratic pieces with sides of about 5 mm were cut out, glued with the coating side onto a flat and stiff steel surface, ground and polished until the ratio of the coating thickness and the thickness of the remaining substrate material was close to 1/100. To avoid stress by grinding and polishing, this was conducted in steps with successive finer grains, finalizing using 1/4 μm diamond. After polishing, the glue was dissolved and the samples allowed to deflect and relieve the residual stress. The curvature of the stress relieved samples was measured using an optical profiler, NT1100 from WYKO. The equipment was used in its white light vertical scanning interferometry mode. The coating thicknesses was measured using an SEM (Leo 440). The data were then put into Stoney's equation (Eq. 1), where E is elastic modulus, t is thickness, ν is Poisson's

ratio, κ is the inverse of radius of curvature and c and s denotes coating and substrate respectively, to calculate the residual stress in the coating.

$$\sigma = \frac{E_s t_s^2}{6(1-\nu_s) t_c} \kappa \quad [1]$$

RESULTS

Flat samples for determination of the $\Delta H/\sigma_{\text{res}}$ ratio

TiN coating on flat HSS

The hardness of stress relieved pillars, shown in Fig.3, and as-deposited coating were measured to be 23.6 ± 2.4 GPa and 28.4 ± 2.8 GPa, respectively. This gives a hardness difference of 4.8 GPa. The curvature of a polished and stress relaxed sample was measured to 0.63 m giving a compressive residual stress before relaxation of 3.9 GPa.

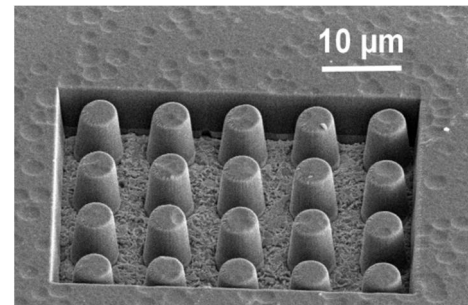


Figure 3. Pillars produced in the TiN coating deposited on a flat HSS substrate.

TiNiC coating on flat nickel substrate

The hardness of stress relieved pillars, shown in Fig. 4, and as-deposited coating were measured to be 17.3 ± 1.7 GPa and 21.2 ± 2.1 GPa respectively. This results in a stress induced hardness increase of 3.9 GPa. The measured curvature of a polished and stress relaxed sample was measured to be 0.12 ± 2.1 m which, with Stoney's equation, suggests a compressive residual stress before relaxation of 2.7 ± 0.3 GPa.

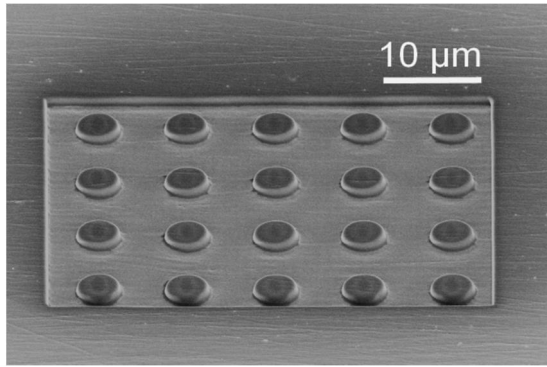


Figure 4. Pillars produced in the TiNiC coating deposited on a flat nickel substrate.

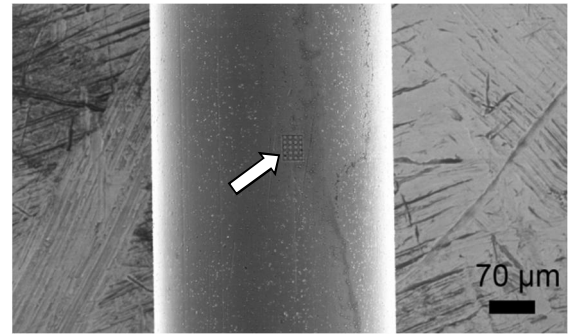


Figure 5. The position of the pillar pattern in the TiN coating deposited on a 0.5 mm stainless steel wire.

The proportionality constants $k = \Delta H / \sigma_{res}$ between the hardness increase and the residual stress were calculated to be 0.81 and 0.69 for the TiN and the TiNiC coatings, respectively.

Investigation of stress conditions on thin wires

As shown in Fig. 5 the area covered by pillars on wires is very small and for all practical reasons the pillars can be assumed to have parallel top surfaces.

The results for the coatings on thin stainless steel wires showed a bit higher hardness both on pillars, shown in Fig. 6, and on as-deposited coatings. The measured hardness for the TiN coating was 27.3 ± 2.7 GPa on the pillars and 32.3 ± 3.2 GPa on the as-deposited coating. For TiN the results were 26.8 ± 2.7 GPa and 29.5 ± 2.9 GPa, respectively. The difference in hardness was calculated to be 5.0 GPa for TiN and 2.7 GPa for the TiNiC coating. In Fig. 7 the two linear curves representing the results from flat specimens are shown. Using the hardness differences as obtained from the wire measurements, the compressive residual stress of the coatings as deposited on wires are shown to be 4.1 GPa for TiN and 1.9 GPa for TiNiC.

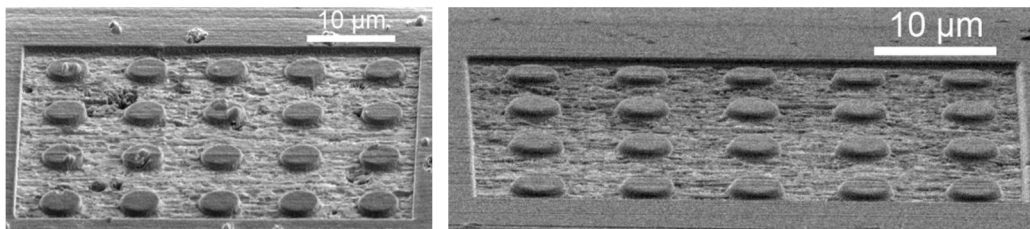


Figure 6. The pillars produced in a) TiN and b) TiNiC. In both coatings milling was conducted until the substrate was reached.

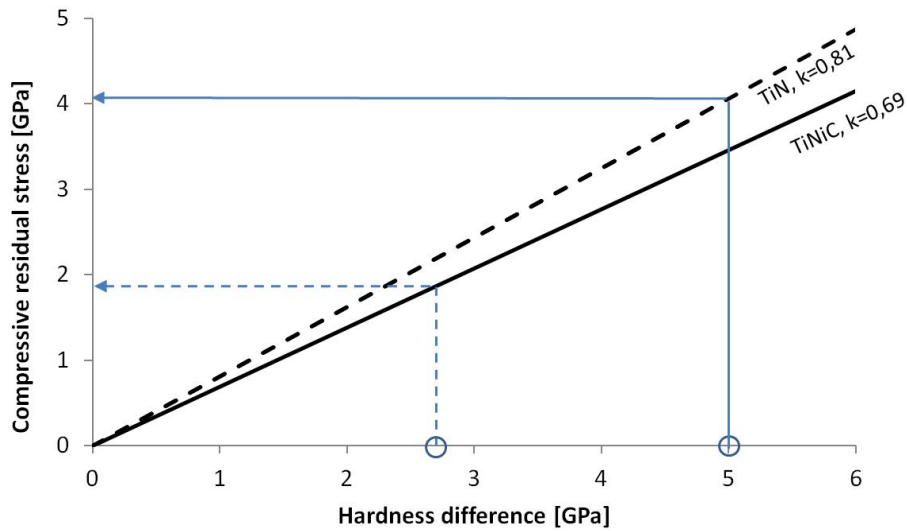


Figure 7. Linear curves from the measurements on flat specimens and the results from the measurements on wire indicated by circles.

DISCUSSION

The results clearly show it is possible to investigate the local residual stress situation by the proposed method. Distinct differences in hardness were measured in the pillars as compared to in as-deposited coating and these differences undoubtedly originate from the stress in the coating.

The lateral residual stress will translate into a hardness contribution differently depending on what material is tested. Both chemical and microstructural differences will influence this and it should thus be expected that different materials, such as crystalline TiN and nanocomposite Ti-Ni-C, will have different proportionality constants, *i.e.* different numerical hardness contributions for a given stress level.

The hardness of the coatings was higher when deposited on thin wires compared to when deposited on flat substrates. Although no temperature measurement of the wires was performed during deposition it is, from thermal conductance reasons, very likely the coatings deposited on wires were grown at higher temperatures than those deposited on

flats. A priori, the resulting higher hardness could be caused by either higher residual stress in the coatings deposited on the wires or by a different structure or chemical composition when deposited on the wires. The results in this work show the residual stress was actually lower for the coatings deposited on the wires and thus chemical and microstructural effects must be the origin of the increased hardness.

The level of uncertainty in the proposed method is on par with XRD and deflection methods. In this procedure, the usual scatter in the hardness measurements is the one dominating factor, although there might be a small influence also from orientation errors like non-horizontal pillar surfaces, during indentation.

For the second part of the method the assumption is made on a linear relation between the hardness increase and the residual stress as suggested by *e.g.* Karlsson et al. [9]. The validity of this assumption must be studied further, especially in cases where coating growth has changed considerably.

FEM calculations suggested a required lower limit of 0.5 in the height/width ratio for acceptable stress relaxation. In this work the pillars were produced close to this lower limit. This was a consequence both of the limited thickness of the coatings, the desire

for easy positioning of the nanoindentations, and results from FEM calculations showing that further milling into the substrate would not have a large effect on stress relaxation, see Fig. 8. However, the validity of this limit *per se* has not been investigated in practice.

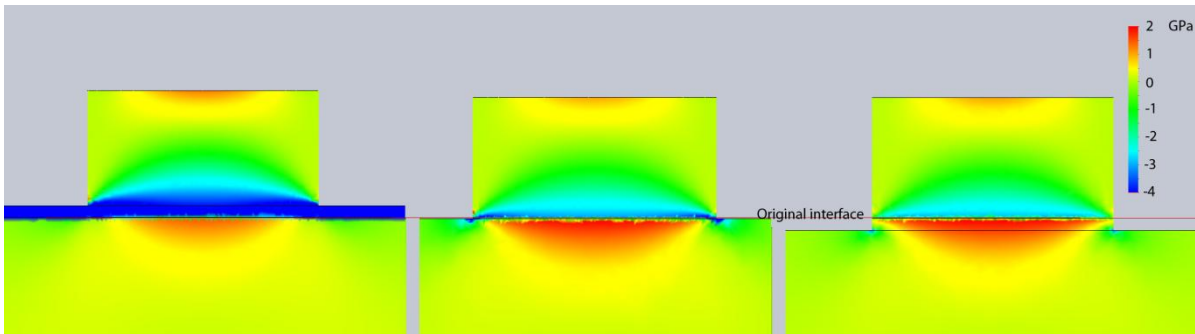


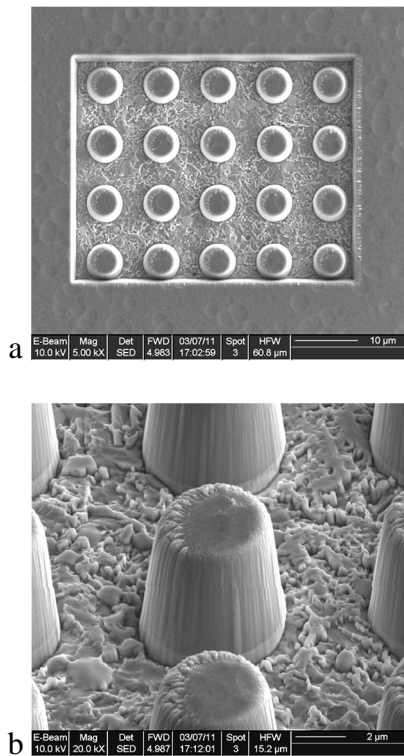
Figure 8. A pillar made to an aspect ratio of 0.5 will relax the compressive stress in the upper part of the pillar, even getting a small tensile stress in the top surface, as shown in the middle figure. Milling slightly short of or beyond the coatings/substrate interface, as shown to the left and right, respectively, would not significantly improve the situation.

The possibilities and exact procedure to produce free standing pillars using FIB is dependent of the system available and the parameters used, just as the quality of the finished pillars is. Using FIB, there is always a risk of re-deposition of material on surrounding surfaces. A small amount of re-deposited material was visible on the pillars on the thickest coating. Most on the sides of the pillars, some also close to the periphery of the pillars but none in the central areas where the indentations were to be conducted see Fig. 9. For the thinner coatings minute amounts of re-deposited material is conceivable but none was detected.

In Fig.9 is also shown that milling was conducted until the substrate was reached. During milling of pillars there is obviously a trade-off between sufficient aspect ratio to allow for adequate stress relaxation, as discussed above and limited amount of milling to minimize the amount of re-deposited material.

Another problem, caused by the material and residual stress themselves, but possibly accentuated by the milling process, is the risk for damaged pillars rendering them unsuitable for indentation experiments. In the TiN coating deposited on wires, four of the pillars were deemed unsuitable for indentation due to either roughness or cracking, *c.f* Fig 6b.

The method for production and hardness measurement of stress relieved coating in micro pillars could possibly be used in combination with other methods for determination of residual stress suggested in the literature. Most suitable is arguably the method proposed by Suresh and Giannakopoulos [5]. This would make their method applicable also to small components with a complex geometry. But the issue of residual stress influence on elastic modulus described by Tsui et al. still remains. More material/substrate combinations, deposition parameters, etc. should be tested to further investigate the possibilities and limitations associated with the micro pillar method.



- Using this method σ_{residual} of TiN and TiNiC on thin wires were calculated to be 4.1 GPa and 1.9 GPa, respectively.
- In this work, the method proved invaluable for deciding the origin of the increase in hardness measured when coatings were deposited on thin wires instead of flat substrates.

ACKNOWLEDGEMENTS

This work was financially supported by Sweden's Innovation Agency, Vinnova, through the program Designade Material.

Figure 9 a) Overview and close-up of one of the micro pillars showing re-deposited material on the sides and the periphery of the top surface but not in the area of nanoindentation.

CONCLUSIONS

The results from this work show that:

- The method readily allows determination of the inherent hardness of stress free coating and any difference in hardness due to the residual stress.
- For TiN on a flat HSS substrate 4.8 GPa of its 28.4 GPa hardness originated from residual stress. For TiNiC on a flat nickel substrate 3.9 GPa of its 21.2 GPa hardness originate from residual stress.
- Using a linear relation between the hardness increase and the residual stress, the residual stress in a coating deposited on a complex substrate geometry can be calculated.

REFERENCES

- 1 U. Wiklund, M. Bromark, M. Larsson, P. Hedenqvist and S. Hogmark, *Cracking resistance of thin hard coatings estimated by four-point bending*, Surf. Coat. Technol., 91 (1997) 57.
- 2 U. Wiklund, J. Gunnars, and S. Hogmark, Influence of residual stresses on fracture and delamination of thin hard coatings, *Wear*, 232 (1999) 262.
- 3 K. Holmberg, H. Ronkainen, A. Laukkanen, K. Wallin, S. Hogmark, S. Jacobson, U. Wiklund, R. M. Souza, and P. Ståhle, *Residual stresses in TiN, DLC and MoS₂ coated surfaces with regard to their tribological fracture behaviour*, *Wear*, 267 (2009) 2142.
- 4 G.G. Stoney, *The tension of metallic films deposited by electrolysis*, Proceedings of the Royal Society of London. Series A, Containing Papers of a Mathematical and Physical Character (1905-1934) Vol. 82(553) (1909) 172-175
- 5 J. Gunnars and U. Wiklund, Determination of growth-induced strain and thermo-elastic properties of coatings by curvature measurements, *Materials Science and Engineering: A*, 336 (2002) 7
- 6 S. Suresh and A. E. Giannakopoulos, A new method for estimating residual stresses by instrumented sharp indentation, *Acta mater.*, 46 (1998) 5755.
- 7 T. Y. Tsui, W. C. Oliver, and G. M. Pharr, Influences of stress on the measurement of mechanical properties using nanoindentation: Part I. Experimental studies in an aluminum alloy, *J. Mater. Res.*, 11 (1996) 752.
- 8 N. Huber and J. Heerens, On the effect of a general residual stress state on indentation and hardness testing, *Acta Materialia*, 56 (2008) 6205.
- 9 Y.-H. Lee and D. Kwon, Estimation of biaxial surface stress by instrumented indentation with sharp indenters, *Acta Mater* 2004;52:1555.
- 10 L. Karlsson, L. Hultman and J.-E. Sundgren, Influence of residual stresses on the mechanical properties of TiC_xN_{1-x} (x=0, 0.15, 0.45) thin films deposited by arc evaporation, *Thin Solid Films*, 371 (2000) 167.
- 11 E. Lewin, B. André, S. Urbonaite, U. Wiklund and U. Jansson, *Synthesis, structure and properties of Ni-alloyed TiC_x-based thin films*, *J. Mater. Chem.*, 20 (2010) 5950.
- 12 W. C. Oliver and G. M. Pharr, Improved technique for determining hardness and elastic modulus using load and displacement sensing indentation experiments, *J. Mater. Res.*, 7 (1992) 1564.